Aspartate-407 in *Rhodobacter sphaeroides* Cytochrome *c* Oxidase Is Not Required for Proton Pumping or Manganese Binding[†]

Jie Qian,[‡] Wenjun Shi,[§] Michelle Pressler,[§] Curt Hoganson,[§] Denise Mills,[‡] Gerald T. Babcock,[§] and Shelagh Ferguson-Miller*,[‡]

Departments of Biochemistry and Chemistry, Michigan State University, East Lansing, Michigan 48824

Received October 30, 1996; Revised Manuscript Received December 23, 1996[⊗]

ABSTRACT: Several pathways for proton transport in cytochrome *c* oxidase have been proposed on the basis of mutational analysis and X-ray structure: at least one for moving "pumped" protons from the interior to exterior of the membrane and a separate route for transporting "substrate" protons from the interior to the binuclear metal center to combine with oxygen to make H_2O. According to the crystal structures of cytochrome *c* oxidase, Asp407 (*Rhodobacter sphaeroides* numbering) is at the interface of subunit I and subunit II of the oxidase, in a negative patch proposed to be the proton exit site in a pumping pathway, as well as a possible ligand to Mg [Iwata et al. (1995) *Nature 376*, 660−669]. Three mutants at the Asp407 position of *R. sphaeroides* cytochrome oxidase, Asp407Ala, Asp407Asn, and Asp407Cys, have been purified and characterized. All showed electron transfer activity, and pH dependence of activity, similar to that of the wild type enzyme and no major structural changes, as evidenced by visible, EPR, and resonance Raman spectroscopy. When reconstituted into artificial vesicles, the purified mutants pumped protons with normal efficiency and responded to the membrane pH and electrical gradients in a manner similar to that of wild type. Furthermore, the EPR spectra and Mn quantitation analysis of mutants grown in high Mn indicated no significant alteration in the Mn/Mg site. These results suggest that Asp407 does not play a critical role in proton translocation or in Mn/Mg binding.

The mechanism of coupling of electron transfer to proton pumping is a major unsolved problem in understanding cytochrome *c* oxidase. A model for a proton pump is provided by bacteriorhodopsin (Krebs & Khorana, 1993), in which a hydrogen-bonded relay system is suggested to be important for proton movement, from theoretical considerations (Nagle & Morowitz, 1978) and from structural and spectral analysis (Henderson et al., 1990; Rothschild, 1992). Thus residues that can participate in hydrogen bonding are of particular interest for mutational analysis of proton pathways. In previous studies, Asp132 in an interior loop between helix II and helix III of subunit I of *Rhodobacter sphaeroides* oxidase was mutated to alanine and asparagine. The mutants showed no proton pumping but retained some electron transfer activity, leading to the proposal that this residue provided the entry site in a proton pumping pathway (Fetter et al., 1995). Similar results were obtained with mutants of the homologous cytochrome bo_3 in *Escherichia coli* (Thomas et al., 1993b; García-Horsman et al., 1995). In agreement with this idea, two possible proton pathways have been identified in the crystal structure of *Paracoccus denitrificans* cytochrome *c* oxidase (Iwata et al., 1995), which shows that Asp132 is on the interior side and in a good position to load protons for pumping. Iwata and colleagues also propose that another acidic amino acid, Asp407, located in an exterior loop between helix IX and helix X of subunit I, could be part of a proton exit path. In the crystal structure of the mammalian enzyme, Yoshikawa and colleagues (Tsukihara et al., 1996) also identify Asp132 as a possible entry site for protons to be pumped but do not invoke Asp407 as an exit site. However, both the *P. denitrificans* and mammalian oxidase crystal structures show Asp407 at the interface of subunit I and subunit II in a negative patch near a proposed Mn/Mg site, between Cu_A and Cu_B (Figure 1). In this study we examined the effects of three different mutations at the Asp407 position on electron transfer, proton pumping, Mn/Mg binding, and Cu_A structure. The results suggest that a carboxyl group at this position is not critical for any of these structural or functional properties of cytochrome *c* oxidase.

MATERIALS AND METHODS

The Asp407Ala/Asn/Cys mutants were made by PCR[1] overlapping extension methods (Ho et al., 1989). Oligo primers of 18−21 bp were synthesized. For each mutant, four primers were used for the polymerase chain reaction, and plasmid DNA pJS3 which contains the COXI gene was used as the template. The 523 bp PCR products containing mutations were digested with *Bgl*II/*Sph*I, and the 352 bp *Bgl*II−*Sph*I fragment was subcloned to plasmid pJS3-X6H which has six histidines tagged to the C-terminus of COXI gene (Mitchell & Gennis, 1995). The *Bgl*II−*Sph*I region of pJS3-X6H of all the mutants was sequenced to confirm the

[†] Supported by National Institutes of Health Grants GM 26916 (to S.F.-M.) and GM 25480 (to G.T.B.).

* Author to whom the correspondence should be addressed. Telephone, 517-355-0199; Fax, 517-353-9334; E-mail, fergus20@pilot.msu.edu.

[‡] Department of Biochemistry, Michigan State University, East Lansing, MI 48824-1319.

[§] Department of Chemistry, Michigan State University, East Lansing, MI 48824.

[⊗] Abstract published in *Advance ACS Abstracts,* February 1, 1997.

[1] Abbreviations: CCCP, carbonyl cyanide *m*-chlorophenylhydrazine; RCR, respiratory control ratio; val, valinomycin; CO, carbon monoxide; PCR, polymerase chain reaction; EPR, electron paramagnetic resonance.

S0006-2960(96)02721-3 CCC: $14.00

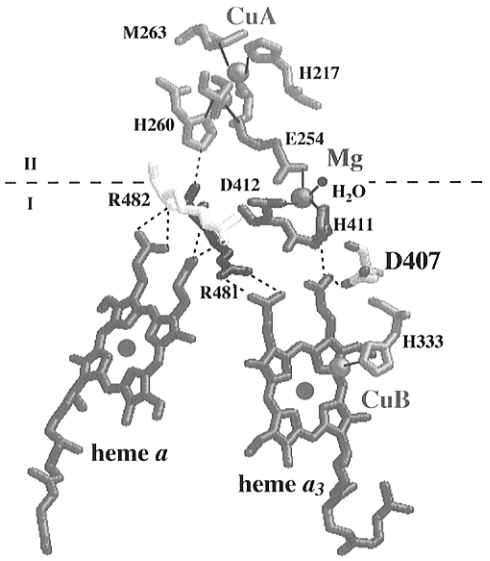

FIGURE 1: Structure of the interface between subunit I and subunit II of beef heart cytochrome *c* oxidase [in *R. sphaeroides* oxidase numbering; coordinates are from Tsukihara et al. (1996), with permission of the authors]. The solid lines indicate the bonds between metals and their ligands. The dashes lines indicate hydrogen bonds. Asp407, His 411, and Asp412 are on the loop between helix IX and helix X in subunit I.

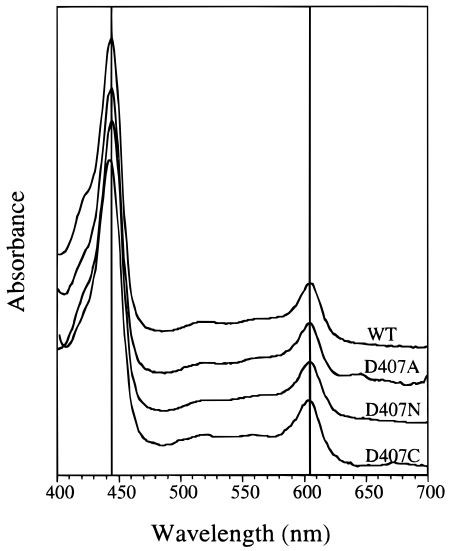

FIGURE 2: Comparison of visible spectra of purified wild type and mutant cytochrome aa_3 of *R. sphaeroides*. Dithionite-reduced absolute spectra of the purified enzyme were recorded with a Perkin-Elmer Lamda 6 UV−visible spectrophotometer at 25 °C. The assay solution includes 100 mM KH_2PO_4, pH 7.2, 0.2% lauryl maltoside, and (A) 0.6 μM Asp407Ala, (B) 0.3 μM Asp407Cys, (C) 0.7 μM Asp407Asn, and (D) 2 μM wild type cytochrome aa_3.

mutation, and no secondary mutations were found. The pJS3-X6H with the mutation was subject to digestion with *Eco*RI/*Hin*dIII. This fragment was subcloned to plasmid pRK415-1, followed by transformation into the *E. coli* strain S17-1, which is capable of conjugating with *R. sphaeroides* strain JS100, a COXI-deleted strain. Single conjugants were grown on Sistrom's plates with antibiotics spectinomycin (50 μg/mL), streptomycin (50 μg/mL), and tetracycline (1 μg/mL) at 30 °C for 2−3 days.

All mutant *R. sphaeroides* cells were grown in Sistrom's medium as described (Hosler et al., 1992) except different Mn and Mg concentrations are indicated in the figure legends.

Mutants were purified with Ni-NTA agarose affinity chromatography (Mitchell & Gennis, 1995) with modifications. All steps were carried out at 4 °C. Cells were resuspended in 50 mM KH_2PO_4, pH 7.2, followed by two passages through a French pressure cell at 20 000 psi. Whole cells and debris were removed by centrifugation at 20 000*g* for 20 min. The supernatant which contains the membranes was pelleted by centrifugation at 200000*g* for 1.5 h. The membranes were homogenized in 10 mM Tris and 40 mM KCl, pH 8.0, and solubilized in 3% lauryl maltoside. The solution was stirred for 1 h. The solubilized membranes were centrifuged at 200000*g* for 30 min. The amount of cytochrome aa_3 was estimated from the dithionite-reduced minus ferricyanide-oxidized spectrum. Imidazole was added to the solubilized membrane (at 0.7 mg of cytochrome aa_3/mL) to a final concentration of 10 mM. Packed resin (0.7 mL)/mg of oxidase was added, and the mixture was stirred for 1 h. The mixture was loaded into a gravity-flow column. The column was washed with 10 column volumes of 10 mM imidazole, 0.1% lauryl maltoside, 10 mM Tris, and 40 mM KCl, pH 8.0, followed by 5 column volumes of 0.1% lauryl maltoside, 10 mM Tris, and 40 mM KCl, pH 8.0. The oxidase was eluted with 100 mM histidine, 0.1% lauryl maltoside, 10 mM Tris, and 40 mM KCl, pH 8.0.

Reconstitution of oxidase into phospholipid vesicles was conducted as described (Fetter et al., 1995).

For the mutants grown in high Mn (700 μM) and low Mg (50 μM), adventitiously bound Mn was removed by incubating the purified enzymes in 50 mM EDTA for 30 min at 4 °C (Hosler et al., 1995), and the oxidase was separated from EDTA by running through a G-75 column. Electron transfer, proton pumping, CO binding, and EPR spectroscopy were measured as described (Hosler et al., 1992).

Resonance Raman spectra were measured as described (Mitchell et al., 1996), except that the excitation wavelength is 438.4 nm, and an average of six scans is shown.

Quantitation of the bound Mn was performed as described (Hosler et al., 1995), except that the spectra were taken on a Bruker ESP300E.

RESULTS

Visible Spectra, Electron Transfer, and CO Binding Assays. Visible spectra of these mutants show that they are highly pure of cbb_3 oxidase and have spectral characteristics similar to those of wild type, although there is a slight blue shift in the α band and Soret band (less than 1 nm; see Figure 2). Purified Asp407Ala, Asp407Cys, and Asp407Asn mutants have 1100, 650, and 1400 s^{-1} activities, which are 85%, 50%, and 100% of wild type oxidase activity, respectively (Table 1). The activities of reconstituted mutants are 700, 550, and 700 s^{-1} for Asp407Ala, Asp407Cys, and Asp407Asn, respectively, compared to 1200 s^{-1} for wild type. The activities after the reconstitution are lower than the activities before the reconstitution, partly because the assay conditions for the reconstituted enzyme are not optimal for maximal activity and, in this case, the mutants may have lesser stability than wild type during the long dialysis. Other possibilities to explain the loss of activity include a different sensitivity to pH or less of the enzyme reconstituted in the correct orientation. The pH dependence of the activity of purified Asp407Ala was compared to wild type over the pH range 6.0−9.0, and a similar pH profile was found (Figure 3).

Table 1: Comparison of Wild Type and Mutant *R. sphaeroides* Cytochrome *c* Oxidase: Electron Transfer Activity of Purified and Reconstituted Enzyme, Respiratory Control Ratios, Proton Pumping Activity, and CO Binding Efficiency

oxidase	activity of purified enzyme (s^{-1})	activity of reconstituted enzyme (s^{-1})	RCR (+val + CCCP)	H^+/e^-	% CO binding (compared to wild type)
wild type	1300 ± 400	1200 ± 300	9	0.5−0.8	100
D407A	1100	700	7	0.7−0.8	100
D407C	650	550	9	0.4−0.6	70
D407N	1400	700	7	0.6	90

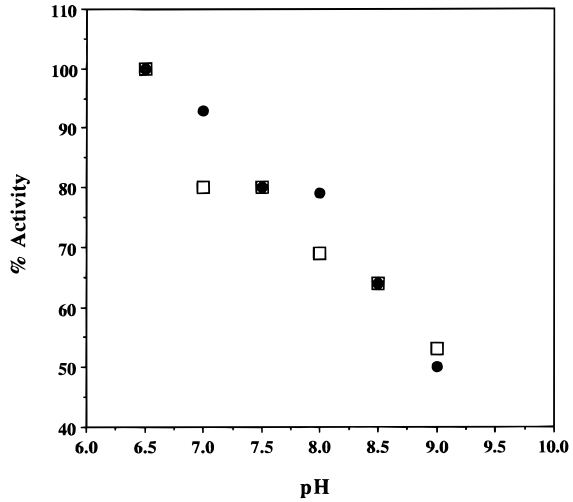

FIGURE 3: pH dependence of activity of purified wild type (□) and Asp407Ala (●) cytochrome *c* oxidase. Activities were assayed polarographically using 0.002 μM Asp407Ala and 0.006 μM wild type in 50 mM potassium phosphate for pH 6.5−7.5 and in 50 mM Tris for pH 7.5−9.0, including 2.8 mM ascorbate, 0.056% lauryl maltoside, 2 mg of cholate-solubilized soybean phospholipid, and 1.1 mM TMPD. Relative activities were calculated as a percent of the highest turnover measured: for wild type (1050 s^{-1}) and for Asp407Ala (1200 s^{-1}).

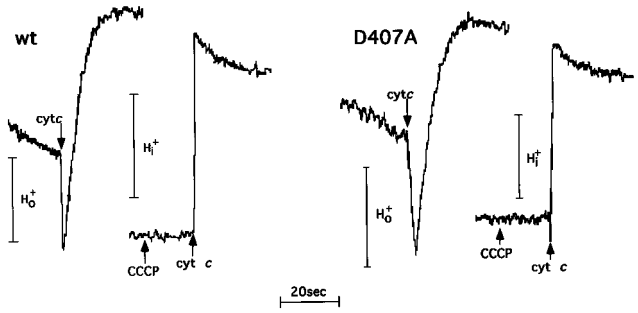

FIGURE 4: Proton pumping activity assay of reconstituted wild type and Asp407Ala cytochrome *c* oxidase. The extravesicular pH change was measured at 556.8 minus 504.7 by phenol red at 22 °C with an Aminco DW2a spectrophotometer. Wild type (A) and mutant Asp407Ala (B) cytochrome *c* oxidase (0.065 nmol) was reconstituted into soybean phospholipid vesicles, which were added in 2.5 mL of assay solutions containing 50 μM $NaHCO_3$, 45 mM KCl, 44 mM sucrose, and 50 μM phenol red, pH 7.4, followed by equilibration with 3.2 μM valinomycin and 0.4 nM CCCP. Rapid acidification was detected upon addition of 0.8 nmol of cytochrome *c* (0.32 μM in final concentration). After addition of 5 μM CCCP and the same amount of cytochrome *c*, pure alkalinization was detected. HCl standard acid (0.5 nmol) was added before (H_o^+) and after (H_i^+) addition of concentrated CCCP. The measurements of H_o^+, H_i^+, and the pure alkalinization were used to calculate the electron transferred (e^-) and the H^+/e^- ratio can be calculated from the electron transferred (e^-) and acidification (H^+). Other mutants have similar proton pumping activity as Asp407Ala (data not shown).

After bubbling 1 mL of CO into dithionite-reduced cytochrome aa_3, 100% of Asp407Ala, 70% of Asp407Cys, and 90% of Asp407Asn are converted to the CO-bound form, compared to 100% for wild type under these conditions. This indicates that no major conformational change has occurred at the binuclear center (Table 1). Asp407Cys has the lowest activity before and after reconstitution and the lowest CO binding among all the mutants, suggesting that a cysteine at this position may have additional detrimental effects unrelated to the loss of a carboxyl, such as seeking a more hydrophobic environment or forming a disulfide bond with another cysteine residue, either of which could lead to structural instability.

Respiratory Control and Proton Pumping. The respiratory control ratio (RCR) is a measure of the completeness of reconstitution and intactness of the artificial membrane vesicles, as well as the innate properties of the mutant oxidase. In the reconstituted oxidase vesicles, an increase of oxygen consumption is expected after addition of the ionophore valinomycin or uncoupler CCCP, due to their ability to release the inhibiting effect of an electrical or proton gradient which is formed when activity is stimulated by addition of cytochrome *c*. The RCR's (activity after ionophore addition divided by activity before) of Asp407Ala, Asp407Cys, and Asp407Asn are 7, 9, and 7, very close to that of wild type (Table 1). When proton pumping is measured using the pH-sensitive dye phenol red, acidification is observed, followed by alkalinization due to consumption of protons to make H_2O in the vesicle interior (Figure 4). The H^+/e^- ratio ranges from 0.4 to 0.8 for the Asp407 mutants, while the wild type has an H^+/e^- ratio of 0.5−0.8, indicating that removal of the carboxyl causes no significant change in proton pumping efficiency, within the accuracy of the assay.

Mn and Cu_A Binding Sites. Cytochrome *c* oxidase contains two copper ions at the Cu_A site and, under certain growth conditions (Hosler et al., 1995), close to stoichiometric Mn. Both metals give unique, quantifiable EPR signals. When *R. sphaeroides* is grown with high Mn (700 μM) and low Mg (50 μM), Mn appears to be inserted into what is normally a Mg site, and the strong Mn EPR signal in the $g = 2.0$ region masks the Cu_A signal. However, under growth conditions of high Mg (1200 μM) and low Mn (0.5 μM), the EPR spectrum of oxidase shows only the Cu_A signal, due to the fact that Mn content of the purified oxidase is below the detection level of EPR spectroscopy and the site is presumably occupied with EPR-silent Mg. When *R. sphaeroides* is grown with high Mg (1200 μM) and medium Mn (27 μM), both Mn and Cu_A signals show in the EPR spectrum of the purified oxidase. Wild type and mutants were grown under the three different conditions, and EPR spectra at 10 K are shown in Figure 4. Under low Mn/high Mg growth conditions, no Mn is bound in wild type or mutant Asp407Ala, revealing a normal Cu_A signal for the mutant (Figure 5A). In the high Mg/medium Mn growth condition, both wild type and mutant Asp407Ala reveal

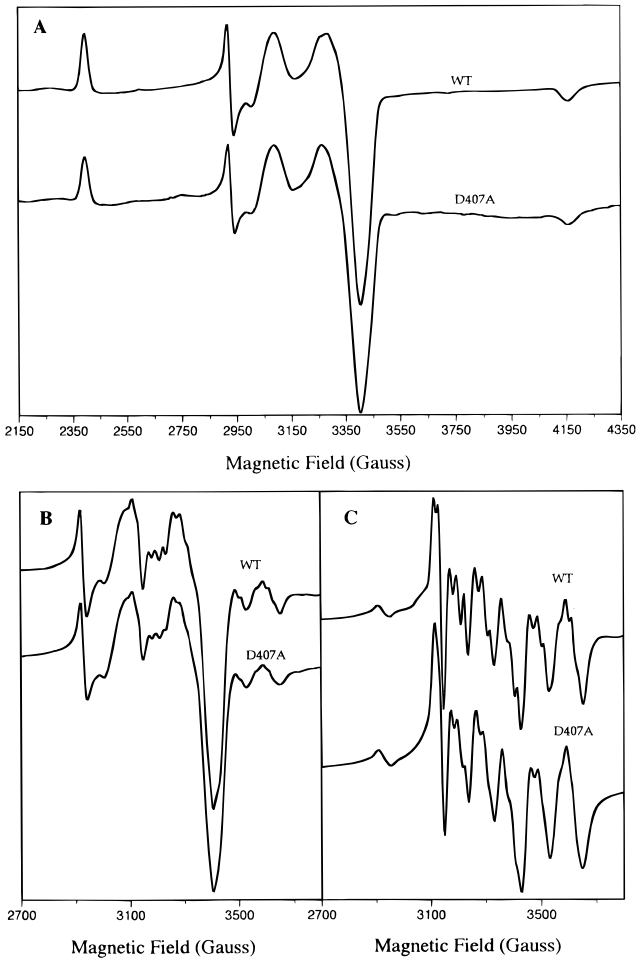

FIGURE 5: EPR spectra of purified wild type and Asp407Ala mutant *R. sphaeroides* cytochrome *c* oxidase grown in (A) high [Mg] (1200 μM) and low [Mn] (0.5 μM), (B) high Mg (1200 μM) and medium Mn (27 μM), and (C) high [Mn] (700 μM) and low [Mg] (50 μM). EPR spectra of Mn were shown at $g = 2.0$ region. The spectra were recorded on a Bruker ESP300E series spectrometer by using a TE_{102} cavity, at X-band at 10 K. Purified mutants (0.3 mL) were used for each EPR spectrum (data of Asp407Asn and Asp407cys are not shown).

similar signals for Cu_A and Mn (Figure 5B), although a slight broadening of the Mn lines is observed in the mutant compared to wild type, leading to an attenuated Mn signal. At high Mn/low Mg growth conditions, both the Asp407Ala mutant and wild type show the typical six-line hexaqua Mn^{2+} spectral characteristics in the $g = 2.0$ region (Figure 5C), suggesting that mutation at the 407 position does not change the Mn ligand structure. Slight broadening is also observed in this signal, indicative of some minor increase in disorder in the Mn binding site. The Mn content was quantified by acidifying and precipitating the protein and comparing the Mn signal to a set of quantitation standards. Under high Mn/low Mg conditions, purified wild type and mutant Asp407Ala oxidases showed similar Mn incorporation, 88% and 85% of stoichiometric, respectively.

Resonance Raman Spectroscopy. The resonance Raman spectra of Asp407Ala and Asp407Asn are identical to wild type in both the high and low frequency region, indicating undisturbed heme *a* and a_3 environments (Figure 6). However, Asp407Cys has about a 50% decrease in intensity at 214, 365, and 1661 cm^{-1} (data not shown), revealing a

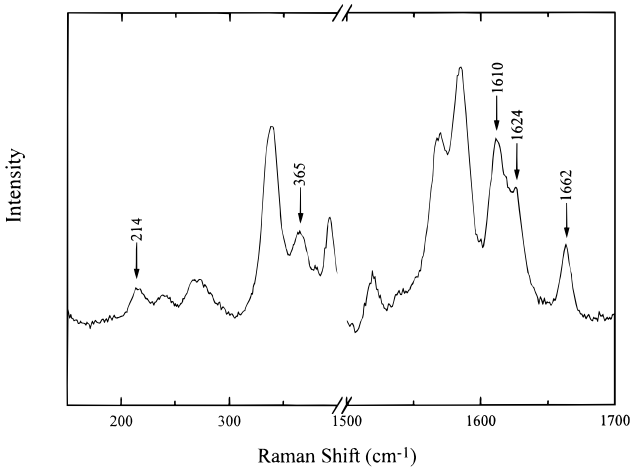

FIGURE 6: Resonance Raman spectrum of purified Asp407Ala cytochrome *c* oxidase. Asp407Ala (67 μM) was reduced with dithionite, and the spectrum was taken at 438.4 nm excitation. The indicated modes are 214 cm^{-1}, $Fe-N_{His}$ stretch of heme a_3; 365 cm^{-1}, ring bending of heme a_3; 1611 cm^{-1}, formyl stretch of heme *a*; 1624 cm^{-1}, vinyl stretch of heme *a*; 1662 cm^{-1}, formyl stretch of heme a_3.

significant effect on the heme a_3 environment that may relate to partial denaturation and lower activity of this mutant.

DISCUSSION

Previous data demonstrated that aspartate-132 is critical for proton pumping activity in both *R. sphaeroides* cytochrome aa_3 (Fetter et al., 1995) and *E. coli* cytochrome bo_3 (Thomas et al., 1993b). It is located on the interior of the membrane in a position that makes it a good candidate for an entry site for protons to be pumped (Iwata et al., 1995; Tsukihara et al., 1996). For understanding the mechanism of coupling between proton translocation and the oxygen chemistry, it is also important to define the exit site for protons. An exit site in close proximity to the binuclear center where the oxygen chemistry occurs would support the idea of direct coupling between these processes, whereas proton efflux at a distance from that region might encourage consideration of an indirect, conformational coupling model.

Aspartate-407, an acidic residue in subunit I, is located in a negatively charged cluster at the interface between subunit I and subunit II, immediately above the heme a_3-Cu_B center (Figure 1). In the context of a direct coupling mechanism, Iwata et al. (1995) suggest Asp407 as a possible proton exit site. The crystal structure also shows that Asp407 is close to the Mn/Mg ligands, His411 and Asp412, identified by mutational analysis (Hosler et al., 1995) and by analysis of the mammalian crystal structure (Tsukihara et al., 1995). In the bacterial enzyme structure, Iwata and colleagues suggest Asp407 as a possible Mg ligand itself. If either of these suggested roles is correct, substitutions at this position might be expected to alter either proton pumping or Mn/Mg binding, or both.

The visible spectra of mutants Asp407Ala, Asp407Cys, and Asp407Asn show that the α band of all the mutants has a maximum at 605 nm, similar to wild type oxidase, except for Asp407Cys (604 nm). In addition, CO binding analysis shows that all substitutions except cysteine retain high efficiency of CO binding. These results suggest that replacement of a negatively charged residue with a neutral residue at this position does not alter the environment at the

heme a_3-Cu_B redox center and imply that the charge at this position is not critical for stabilizing the protein structure.

The oxygen consumption assay of the purified mutants shows that they all have high activity, approaching that of wild type, except Asp407Cys, which is only ~50% active. A cysteine at this position may interact in some way to destabilize the protein, by seeking a more apolar environment or forming an inter- or intramolecular disulfide bond. From the crystal structure, possible candidates would be Cys64, Cys88 in the loop between helix I and helix II of subunit I, or a cysteine in subunit II that ligates Cu_A.

All mutants pump protons with efficiency similar to that of wild type, indicating that Asp407 is not required for proton translocation. A new model proposed by Tsukihara et al. (1996) suggests two possible pumped proton channels, in addition to a channel for substrate protons. Since neither of these pumping pathways accesses the binuclear center, they imply an indirect coupling of electron transfer to proton translocation involving a conformational change driven by the oxygen chemistry, but at a distance from the active site (Tsukihara et al., 1996). The lack of effect of the Asp407 mutations on proton pumping efficiency, or pH dependence of activity, is consistent with this model in that this residue is not predicted to be a part of either of the proposed "indirect" channels. However, these results certainly do not rule out the histidine cycle/shuttle model (Wikström et al., 1994; Iwata et al., 1995) since any one of a number of residues, or bound water in the region above the active site, could be involved in proton efflux.

EPR data show that Asp407 is not required for Mn binding, although it is close to the two proposed Mg/Mn ligands, His411 and Asp412. The similar spectral characteristics and content of bound Mn in wild type and the Asp407Ala mutant grown in high Mn indicate that this carboxyl does not play a critical role at the Mn/Mg site. The observed broadening of the Mn signal could be related to removal of its hydrogen bond to the His411 ligand. The spectra also show that the Cu_A site is not changed by substitution, suggesting that this residue is not critical for maintaining the interface of subunits I and II where the Cu_A and Mg are located.

The heme environments are not changed by replacing aspartate with alanine or asparagine, which confirms that neither the carboxylate function nor the hydrogen-bonding capacity of this residue is structurally critical. The altered heme a_3 environment of Asp407Cys seen by resonance Raman is in agreement with shifted visible spectra, lower CO binding, and lower activity and suggests that the presence of cysteine causes some destabilization of the heme a_3-Cu_B center, such that some proportion of the enzyme, 5−50% depending on the assay conditions, can become denatured.

In conclusion, all the data in this study show that aspartate-407 is not a critical residue in cytochrome *c* oxidase for proton pumping, for Mn binding, or for maintaining protein structure at the subunit I/II interface. Other residues may be capable of substituting for its function in a proton (Iwata et al., 1995) or water exit channel (Tsukihara et al., 1996), but the lack of effect on Mn spectral characteristics and binding is strong evidence that it is not a Mn/Mg ligand.

ACKNOWLEDGMENT

We thank S. Yoshikawa for generous permission to use the figure of the structure of the interface between subunit I and subunit II of beef heart cytochrome *c* oxidase, derived from the X-ray coordinates.

REFERENCES

Fetter, J. R., Qian, J., Shapleigh, J., Thomas, J. W., García-Horsman, J. A., Schmidt, E., Hosler, J., Babcock, G. T., Gennis, R. B., & Ferguson-Miller, S. (1995) *Proc. Natl. Acad. Sci. U.S.A. 92*, 1604−1608.

García-Horsman, J. A., Puustinen, A., Gennis, R. B., & Wikström, M. (1995) *Biochemistry 34*, 4428−4433.

Henderson, R., Baldwin, J. M., Ceska, T. A., Zemlin, F., Beckmann, E., & Downing, K. H. (1990) *J. Mol. Biol. 213*, 899−929.

Ho, S. N., Hunt, H. D., Horton, R. M., Pullen, J. K., & Pease, L. R. (1989) *Gene 77*, 51−59.

Hosler, J. P., Fetter, J., Tecklenburg, M. M. J., Espe, M., Lerma, C., & Ferguson-Miller, S. (1992) *J. Biol. Chem. 267*, 24264−24272.

Hosler, J. P., Espe, M. P., Zhen, Y., Babcock, G. T., & Ferguson-Miller, S. (1995) *Biochemistry 34*, 7586−7592.

Iwata, S., Ostermeier, C., Ludwig, B., & Michel, H. (1995) *Nature 376*, 660−669.

Krebs, M. P., & Khorana, H. G. (1993) *J. Bacteriol. 175*, 1555−1560.

Mitchell, D. M., & Gennis, R. B. (1995) *FEBS Lett. 368*, 148−150.

Mitchell, D. M., Ädelroth, P., Hosler, J. P., Fetter, J. R., Brzezinski, P., Pressler, M. A., Aasa, R., Malmström, B. G., Alben, J. O., Babcock, G. T., Gennis, R. B., & Ferguson-Miller, S. (1996) *Biochemistry 35*, 824−828.

Nagle, J. F., & Morowitz, H. J. (1978) *Proc. Natl. Acad. Sci. U.S.A. 75*, 298−302.

Rothschild, K. J. (1992) *J. Bioenerg. Biomembr. 24*, 147−167.

Thomas, J. W., Puustinen, A., Alben, J. O., Gennis, R. B., & Wikström, M. (1993b) *Biochemistry 32*, 10923−10928.

Tsukihara, T., Aoyama, H., Yamashita, E., Tomizaki, T., Yamaguchi, H., Shinzawa-itoh, K., Nakashima, R., Yaono, R., & Yoshikawa, S. (1995) *Science 269*, 1069−1074.

Tsukihara, T., Aoyama, H., Yamashita, E., Tomizaki, T., Yamaguchi, H., Shinzawa-Itoh, K., Nakashima, R., Yaono, R., & Yoshikawa, S. (1996) *Science 272*, 1136−1144.

Wikström, M., Bogachev, A., Finel, M., Morgan, J. E., Puustinen, A., Raitio, M., Verkhovskaya, M. L., & Verkhovsky, M. I. (1994) *Biochim. Biophys. Acta 1187*, 106−111.

BI962721+